Journal of Magnetic Resonance **149,** 52–57 (2001)
doi:10.1006/jmre.2000.2269, available online at http://www.idealibrary.com on IDEAL®

COIN TACSY, a Novel Approach to Tailored Correlation Spectroscopy

Teresa Carlomagno,*,† Thomas Prasch,*,[1] and Steffen J. Glaser‡,[2]

*Institut für Organische Chemie, J. W. Goethe-Universität, Marie-Curie-Strasse 11, D-60439 Frankfurt, Germany; †Department of Molecular Biology, and the Skaggs Institute of Chemical Biology, The Scripps Research Institute, MB 33, 10550 North Torrey Pines Road, La Jolla, California 92037; and ‡Institut für Organische Chemie und Biochemie II, Technische Universität München Lichtenbergstrasse 4, D-85747 Garching, Germany

Received August 11, 2000

A new class of frequency-selective homonuclear Hartmann–Hahn mixing sequences has been developed. These tailored correlation experiments are based on a combination of isotropic mixing and selective nutation (COIN). Compared to previous approaches, the new mixing sequences offer improved sensitivity and considerably more flexibility concerning the choice of the active frequency ranges. © 2001 Academic Press

Key Words: **TOCSY; TACSY; homonuclear Hartmann–Hahn transfer; HOHAHA; correlation spectroscopy.**

INTRODUCTION

Homonuclear Hartmann–Hahn transfer (*1–4*) is one of the most widely used experimental building blocks in modern NMR spectroscopy. In the mixing period of TOCSY (total correlation spectroscopy) experiments, isotropic mixing leads to the transfer of coherence and polarization between all spins of a contiguous coupling network. However, for many applications, it can be of advantage to restrict magnetization transfer to a selected subset of spins in the coupling network (*4–9*). This can be achieved using TACSY (tailored correlation spectroscopy) sequences (*4, 5*) that create effective Hamiltonians in which selected spins are decoupled during the mixing process. Some approaches (*10–13*) only reduce undesired isotropic coupling tensors $\mathcal{H}_{kl}^{(I)}$ to so-called longitudinal coupling tensors $\mathcal{H}_{kl}^{(L)}$ (weak coupling) (*4, 5*) rather than completely eliminating them. Although this approach does block Hartmann–Hahn transfer between spins k and l, it also reduces the transfer efficiency of the desired transfer between the remaining spins (*4, 5*). Other approaches (*7, 14, 15*) completely eliminate undesired couplings during the mixing period but also scale down the desired coupling constants by 50%. TACSY experiments that eliminate unwanted couplings without reducing the desired couplings have been realized experimentally using computer-optimized multiple-pulse sequences (*6*). However, these sequences rely on nonvanishing effective spin-lock fields and because of the effects of RF inhomogeneity allow only the efficient transfer of a single magnetization component (e.g., x magnetization) between the spins of interest. Hence, these TACSY sequences do not allow the use of sensitivity-enhancement techniques that rely on the simultaneous transfer of two orthogonal magnetization components (*16*). Here a flexible new approach that makes it possible to create isotropic mixing conditions between selected spins while other spins are fully decoupled is presented. This approach is based on broadband isotropic mixing sequences in combination with band-selective shaped pulses (COIN TACSY: *c*ombination of *i*sotropic mixing and selective *n*utation) for the tailor-made homonuclear decoupling of defined spectral regions.

THEORY

We consider a homonuclear spin system with the Hamiltonian

$$\mathcal{H}_0 = \mathcal{H}_{cs} + \mathcal{H}_J, \qquad [1]$$

where the chemical shift term has the form

$$\mathcal{H}_{cs} = \sum_k 2\pi\,\nu_k I_{kz} \qquad [2]$$

and the scalar coupling term is given by

$$\mathcal{H}_J = \sum_{k<l} 2\pi\, J_{kl} \mathbf{I}_k \mathbf{I}_l = \sum_{k<l} 2\pi\, J_{kl} (I_{kx} I_{lx} + I_{ky} I_{ly} + I_{kz} I_{lz}). \qquad [3]$$

The application of broadband isotropic mixing sequences, such as DIPSI-2 (*17*), reduces the free evolution Hamiltonian $\mathcal{H}_0$ to an effective isotropic mixing Hamiltonian $\mathcal{H}_{eff} = \mathcal{H}_J$ (*2, 4*). In the following discussion we assume that such an isotropic effective Hamiltonian can be created by a first averaging process. In order to optimize coherence transfer it can be desirable to reduce the effective size of the coupling network by eliminating undersired isotropic coupling terms $\mathcal{H}_J^{(u)}$, while desired isotropic coupling terms $\mathcal{H}_J^{(d)}$ are preserved (*4, 5*). This poses the problem of designing a sequence of RF pulses which selectively eliminates undesired isotropic coupling terms $\mathcal{H}_J^{(u)}$ in a second averaging process. For example, consider three coupled spins 1/2 with offsets ν_1, ν_2, ν_3 and nonzero coupling constants J_{12} and J_{23} forming a linear coupling network, where $J_{13} = 0$. In this case, coherence transfer between spins 1 and 2 is most efficient if an effective *IOO*-type coupling topology (*5*) is created, where spins 1 and 2 are isotropically coupled and the

[1] Current address: Zeutrale Analytik, Geb. Z 43, Heukel KGaA, D-40191 Düsseldrof, Germany.

[2] To whom correspondence should be addressed. E-mail: glaser@ch.tum.de.

1090-7807/01 $35.00

coupling term between spins 2 and 3 is completely eliminated. Hence, in this case the term

$$\mathcal{H}_J^{(d)} = 2\pi J_{12}\mathbf{I}_1\mathbf{I}_2 \qquad [4]$$

is desired, whereas the term $\mathcal{H}_J^{(u)} = 2\pi J_{23}\mathbf{I}_2\mathbf{I}_3$ is undesired.

If spins 2 and 3 were only weakly coupled in the effective Hamiltonian resulting from the first averaging process, the application of a train of additional inversion pulses selectively applied to spin 3 would result in complete decoupling of spin 3 in this second averaging process (*18*). For the case of two $180^\circ_x(3)$ pulses with delays τ, the cyclic basis sequence is shown schematically in Fig. 1A. However, in the case of isotropic coupling terms (Eq. [3]) this simple approach fails to provide the desired full decoupling of spin 3. In the toggling frame (*18, 19*) defined by the action of the selective 180°_x pulses, the isotropic mixing Hamiltonian $\tilde{\mathcal{H}}_J(t)$ is given by

$$\tilde{\mathcal{H}}_J(t) = \begin{cases} 2\pi J_{12}\mathbf{I}_1\mathbf{I}_2 + 2\pi J_{23}(I_{2x}I_{3x} + I_{2y}I_{3y} + I_{2z}I_{3z}) \\ \quad \text{for } 0 < t < \tau \\ 2\pi J_{12}\mathbf{I}_1\mathbf{I}_2 + 2\pi J_{23}(I_{2x}I_{3x} - I_{2y}I_{3y} - I_{2z}I_{3z}) \\ \quad \text{for } \tau < t < 2\tau. \end{cases} \qquad [5]$$

The resulting average Hamiltonian

$$\bar{\mathcal{H}}_J = 2\pi J_{12}\mathbf{I}_1\mathbf{I}_2 + 2\pi J_{23}I_{2x}I_{3x} \qquad [6]$$

represents an example of an effective *ILL*-type coupling topology (*5*) in which spin 3 is not completely decoupled and the remaining coupling term $2\pi J_{23}I_{2x}I_{3x}$ reduces the efficiency of coherence transfer between spins 1 and 2 (*4, 5*). The average Hamiltonian $\bar{\mathcal{H}}_J$ is a good approximation of an exact effective Hamiltonian $\mathcal{H}_{eff}$ if $\tau_b \ll 1/J_{kl}$, where $\tau_b = 2\tau$ is the duration of the basic cycle of the second averaging process. Hence, τ_b must be shorter than the inverse of the largest coupling in the spin system. For typical proton–proton coupling constants that are on the order of 10 Hz, this results in the relatively mild condition that the cycle time τ_b of the sequence should be less than 100 ms.

Complete decoupling of spin 3 can be achieved by the sequence shown schematically in Fig. 1B with a cycle time $\tau_b = 4\tau$. This sequence creates the toggling-frame Hamiltonian

$$\tilde{\mathcal{H}}_J(t) = \begin{cases} 2\pi J_{12}\mathbf{I}_1\mathbf{I}_2 + 2\pi J_{23}(I_{2x}I_{3x} + I_{2y}I_{3y} + I_{2z}I_{3z}) \\ \quad \text{for } 0 < t < \tau \\ 2\pi J_{12}\mathbf{I}_1\mathbf{I}_2 + 2\pi J_{23}(I_{2x}I_{3x} - I_{2y}I_{3y} - I_{2z}I_{3z}) \\ \quad \text{for } \tau < t < 2\tau \\ 2\pi J_{12}\mathbf{I}_1\mathbf{I}_2 + 2\pi J_{23}(-I_{2x}I_{3x} - I_{2y}I_{3y} + I_{2z}I_{3z}) \\ \quad \text{for } 2\tau < t < 3\tau \\ 2\pi J_{12}\mathbf{I}_1\mathbf{I}_2 + 2\pi J_{23}(-I_{2x}I_{3x} + I_{2y}I_{3y} - I_{2z}I_{3z}) \\ \quad \text{for } 3\tau < t < 4\tau \end{cases} \qquad [7]$$

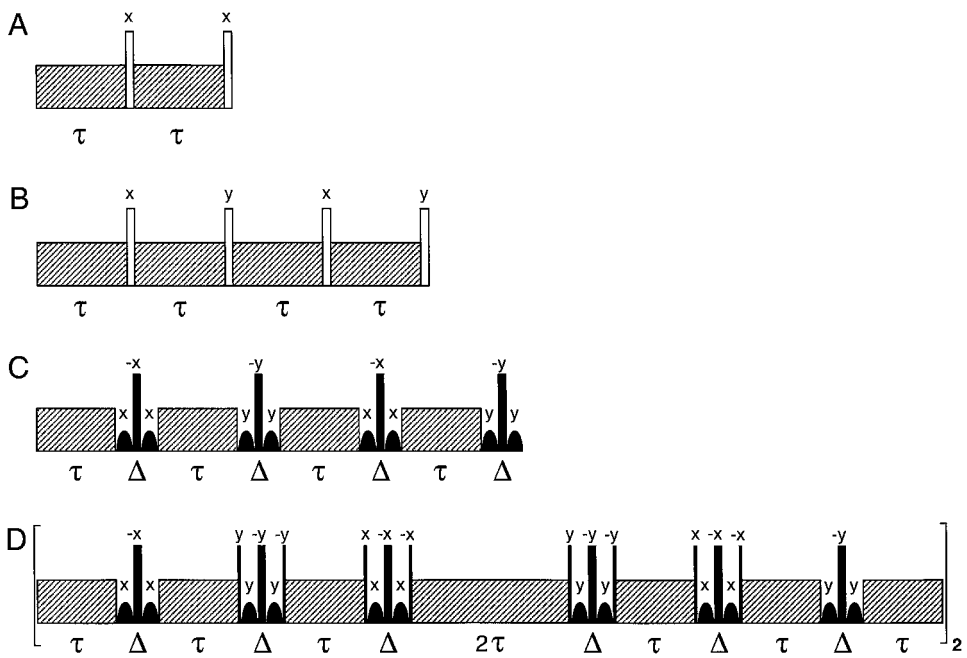

FIG. 1. Schematic representation of COIN TACSY experiments. Hatched boxes represent an isotropic mixing sequence such as DIPSI-2 (*17*). Narrow and wide bars represent 90° and 180° pulses, respectively. In A and B, open bars correspond to idealized selective pulses with neglegible durations. In C an experimental realization of sequence B is shown using combinations of practical selective 90° pulses of finite duration (bell-shaped symbols) and of nonselective pulses (solid bars). An optimized COIN TACSY sequence is shown in D. The cycle times τ_b of the sequences are (A) 2τ, (B) 4τ, (C) $4\tau + 4\Delta$, and (D) $16\tau + 12\Delta$.

with the desired average Hamiltonian

$$\bar{\mathcal{H}}_J = 2\pi J_{12}\mathbf{I}_1\mathbf{I}_2 = \mathcal{H}_J^{(d)}. \quad [8]$$

The undesired coupling term $\mathcal{H}_J^{(u)}$ is completely eliminated, resulting in an effective *IOO*-type coupling topology (*4, 5*). Note that for ideal selective inversion pulses the relative signs of the pulse phases are irrelevant. For example, the cyclic sequence

$$\{\tau\text{–}180^\circ_x(3)\text{–}\tau\text{–}180^\circ_y(3)\text{–}\tau\text{–}180^\circ_x(3)\text{–}\tau\text{–}180^\circ_y(3)\} \quad [9]$$

creates the same $\tilde{\mathcal{H}}_J(t)$ and $\bar{\mathcal{H}}_J$ as the sequence

$$\{\tau\text{–}180^\circ_x(3)\text{–}\tau\text{–}180^\circ_y(3)\text{–}\tau\text{–}180^\circ_{-x}(3)\text{–}\tau\text{–}180^\circ_{-y}(3)\}. \quad [10]$$

However, in the presence of nonideal pulses with inhomogeneous RF fields, these sequences are not equivalent and sequence [9] is preferable. In this sequence, the phase cycle scheme of the selective 180° pulses is equivalent to a robust modified Carr–Purcell sequence indroduced by Maudsley (*20, 21*). Note that the same toggling-frame Hamiltonian $\tilde{\mathcal{H}}_J(t)$ (Eq. [7]) and the same average Hamiltonian $\bar{\mathcal{H}}_J$ (Eq. [8]) also result if the selective pulses are applied simultaneosly to spins 1 and 2, rather than to spin 3; i.e., sequence [9] is also equivalent to

$$\{\tau\text{–}180^\circ_x(1,2)\text{–}\tau\text{–}180^\circ_y(1,2)\text{–}\tau\text{–}180^\circ_x(1,2)\text{–}\tau\text{–}180^\circ_y(1,2)\}. \quad [11]$$

So far we considered ideal selective pulses of neglegible duration. In practice, the finite duration of selective pulses must also be taken into account in the calculation of the average Hamiltonian. In particular, the evolution of chemical shifts and couplings must be considered during the selective inversion pulses. Chemical shift evolution of all spins can be refocused by implementing an ideal selective pulse $180^\circ_x(1, 2)$ as $\{90^\circ_x(3), 180^\circ_x, 90^\circ_{-x}(3)\}$. With this modification, sequence [11] is shown in Fig. 1C. A disadvantage of this implementation is the fact that during the selective inversion elements of duration Δ, spins 1 and 2 are only weakly coupled; i.e., $\mathcal{H}_\Delta^{(12)} = 2\pi J_{12}I_{1z}I_{2z}$. This leads to a nonisotropic average Hamiltonian of the form

$$\bar{\mathcal{H}}'_J = 2\pi J'_{12}(I_{1x}I_{2x} + I_{1y}I_{2y}) + 2\pi J_{12}I_{1z}I_{2z} \quad [12]$$

with a scaled effective coupling constant

$$J'_{12} = \frac{\tau}{\tau + \Delta} J_{12}. \quad [13]$$

The anisotropy caused by the term $\mathcal{H}_\Delta^{(12)} = 2\pi J_{12}I_{1z}I_{2z}$ can be eliminated using additional transformations which also create terms $2\pi J_{12}I_{1x}I_{2x}$ and $2\pi J_{12}I_{1y}I_{2y}$ during subsequent periods Δ. Figure 1D shows such an improved sequence that not only requires less selective inversion periods Δ relative to the number of isotropic mixing periods τ, but also leads to an *isotropic* average Hamiltonian

$$\bar{\mathcal{H}}''_J = 2\pi J''_{12}\mathbf{I}_1\mathbf{I}_2 \quad [14]$$

with a more favorable scaling factor for the effective coupling constant

$$J''_{12} = \frac{4\tau + \Delta}{4\tau + 3\Delta} J_{12}. \quad [15]$$

For example, for $\tau = 10$ ms and $\Delta = 3$ ms, Eq. [13] yields $J'_{12} = 0.769J_{12}$, whereas according to Eq. [15] we find $J''_{12} = 0.878J_{12}$. Hence, compared to the sequence shown in Fig. 1C, the modified sequence of Fig. 1D makes it possible to reduce the transfer time and to achieve a uniform transfer rate for all magnetization components.

The basic pulse sequence element shown in square brackets in Fig. 1D is only cyclic (*18, 19*) up to a $180^\circ_z(1, 2)$ rotation. As indicated in Fig. 1D, the sequence can be made cyclic by applying the basic pulse sequence element twice. However, for relatively short mixing periods, it is also possible to apply the sequence in square brackets only once and to flip the phase of the detected spectrum by 180°, which is equivalent to a nonselective 180°_z rotation. As spin 3 is decoupled, it does not take part in the magnetization transfer dynamics and the resulting phase inversion of the diagonal signal of the third spin can be ignored in practice.

The new COIN TACSY approach has been tested by numerical simulations and experiments using the proton spin system of alanine with offsets $\nu_N = 1075$ Hz, $\nu_\alpha = -1075$ Hz, and $\nu_\beta = -2711.6$ Hz and coupling constants $J_{N\alpha} = J_{\alpha\beta} = 7.5$ Hz. Figure 2 shows characteristic simulated transfer functions of x magnetization for broadband isotropic mixing conditions (Fig. 2A), for the CABBY-1 sequence (*6*) (Fig. 2B), and for the new COIN TACSY sequence shown in Fig. 1D (Fig. 2C). In Fig. 2A, broadband isotropic mixing periods were created using the DIPSI-2 sequence with an RF amplitude of 8.33 kHz, corresponding to a cycle time of 3.453 ms. The band-selective CABBY-1 sequence (Fig. 2B) had an RF amplitude of 3.991 kHz, corresponding to a cycle time of 1.48 ms. In the simulations of the COIN sequence (Fig. 2C), Gaussian pulses with a duration of 1.844 ms (corresponding to $5/\nu_\beta$) and a truncation level of 5% were used for the selective $90^\circ_\varphi(3)$ pulses. In order to minimize pulse imperfections, the nonselective 90°_φ and 180°_φ pulses were implemented by the composite pulses $C(90^\circ_\varphi) = \{24^\circ_\varphi, 152^\circ_{\varphi+\pi}, 346^\circ_\varphi, 152^\circ_{\varphi+\pi}, 24^\circ_\varphi\}$ and $C(180^\circ_\varphi) = \{58^\circ_\varphi, 140^\circ_{\varphi+\pi}, 344^\circ_\varphi, 140^\circ_{\varphi+\pi}, 58^\circ_\varphi\}$ (*22*) with an RF amplitude of 19.8 kHz. The isotropic mixing periods were implemented using DIPSI-2 with an RF amplitude of 11.9 kHz. The period $\tau = 7.25$ ms corresponded to three DIPSI-2 cycles and the basic COIN building block shown in Fig. 1D in square brackets had a duration of 81.4 ms. The simulations were performed using an extended version of the program SIMONE (*23*),

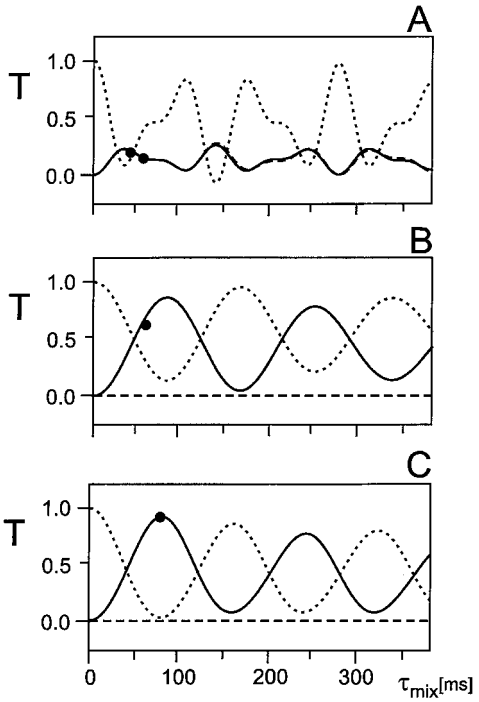

FIG. 2. Simulated transfer functions and experimental transfer amplitudes of x magnetization for the spin system of alanine under (A) broadband isotropic mixing conditions using DIPSI-2 (*17*), (B) the CABBY-1 sequence (*6*), and (C) the new COIN TACSY sequence shown in Fig. 1D. The solid curves represent H_α–H_N transfer, the dashed curves show H_α–H_β transfer, and the dotted curves correspond to H_α–H_α transfer (diagonal signal). The circles represent experimental transfer amplitudes; for experimental details see the text.

neglecting relaxation. RF inhomogeneity has been taken into account, assuming a Gaussian distribution of the RF amplitudes with a full width at half-height of 10% of the nominal RF amplitude. Transfer functions were calculated based on the exact effective Hamiltonian for one cycle. In order to increase the fingerprint signals in the spectrum, a maximum transfer amplitude between H_α and H_N is desirable. Figure 2 shows the desired transfer of x magnetization from H_α to H_N (solid curves). In addition, the transfer of x magnetization from H_α to the individual H_β spins of the methyl group (dashed curves) and the transfer from H_α to H_α (corresponding to the diagonal signal) are shown (dotted curves). As expected, in Figs. 2B and 2C, no transfer is observed between H_α and H_β. The simple transfer characteristics of an effective two-spin system (*4*) consisting of H_α and H_N is approximated best by the COIN TACSY sequence (Fig. 2C), which achieves almost complete coherence transfer from H_α to H_N at a mixing time $\tau_{mix} \approx 80$ ms $\approx 1/(2J_{N\alpha})$. The maximum amplitude of the desired transfer between H_α and H_N is approximately increased by a factor of 4 compared to the TOCSY transfer under broadband isotropic mixing conditions (Fig. 2A).

Figure 2 also shows experimental transfer amplitudes (circles) for the alanine residue of the peptide fragment Gln-Lys-Leu-Glu-Ala-Met-His-Arg-Gln-Lys-Tyr-Pro which is part of the conserved region of the protein encoded by the human Y-located gene SRY (sex-determining region Y) (*6*, *25*). The experimentally determined offsets and coupling constants were identical with the values used in the simulations. The experimental pulse sequence parameters were chosen to roughly match the parameters used in the simulations. In the experimental COIN sequence (Fig. 2C), e-SNOB pulses (*24*) with a duration of 1.468 ms (corresponding to $4/\nu_\beta$) were used for the selective $90^\circ_\varphi(3)$ pulses. The nonselective 90°_φ and 180°_φ pulses were implemented by the same composite pulses (*22*) as in the simulations but with an RF amplitude of 30.5 kHz. The isotropic mixing periods were implemented using DIPSI-2 with an RF amplitude of 8.33 kHz. The period $\tau = 6.9$ ms corresponded to two DIPSI-2 cycles and the basic COIN building block shown in Fig. 1D in square brackets had a duration of 73.8 ms. A good match was found between theoretical and experimental transfer amplitudes.

The isotropy and selectivity of the COIN TACSY approach is demonstrated in Figs. 3A–3C which show the simulated transfer efficiency (*4, 23*) of x, y, and z magnetization for an isolated two-spin system under sequence D of Fig. 1. As expected, no transfer is found to or from spins with offsets between -2 and -3.4 kHz, i.e., near the irradiation frequency at -2.7116 kHz of the selective Gaussian $90^\circ_\varphi(3)$ pulses with a duration of 1.844 ms. Except for this offset range, the offset dependence of the coherence transfer efficiency matches the offset dependence of the DIPSI-2 sequence (*4, 17*). In particular, the transfer of x, y, and z magnetization is almost identical in the entire active bandwidth, demonstrating that the transfer of coherence and polarization is virtually isotropic. This makes it possible to use sensitivity-enhancement techniques that rely on the simultaneous transfer of two orthogonal magnetization components (*16*). Sensitivity-enhanced 2D TOCSY and TACSY experiments were acquired of the peptide fragment Gln-Lys-Leu-Glu-Ala-Met-His-Arg-Gln-Lys-Tyr-Pro. The experimental parameters were identical to the parameters for the experimental results shown in Fig. 2. Representative NH–H_α cross peaks of the Leu, Ala, Arg, and Tyr residues of the peptide are shown in Fig. 4. The mixing sequence of the sensitivity-enhanced TOCSY experiment was DIPSI-2 with a duration of 44.9 ms (dashed traces in Fig. 4) and 58.7 ms (dashed-dotted traces in Fig. 4). The solid curves represent traces of the sensitivity-enhanced TACSY spectrum with the COIN mixing sequence shown in Fig. 1D and a mixing time of 73.7 ms. In addition, a non-sensitivity-enhanced version of the HNHA-TACSY experiment was acquired using the CABBY-1 sequence with a mixing time of 60.7 ms (*6*). As this mixing sequence only allows the transfer of a single magnetization component, the experimental traces were multiplied by a factor of $\sqrt{2}$ for comparison (dotted traces). In the case of Leu, Ala, and Arg (Figs. 4A–4C), the H_β protons were covered by the selective 90° pulses of the COIN sequence. As expected, the sensitivity-enhanced COIN TACSY peaks are between a factor of 1.8 and 3.3 more intense than the corresponding peaks in the broadband TOCSY sequence. No advantage of the COIN experiment is found for the Tyr residue (Fig. 4D) because the H_β protons were

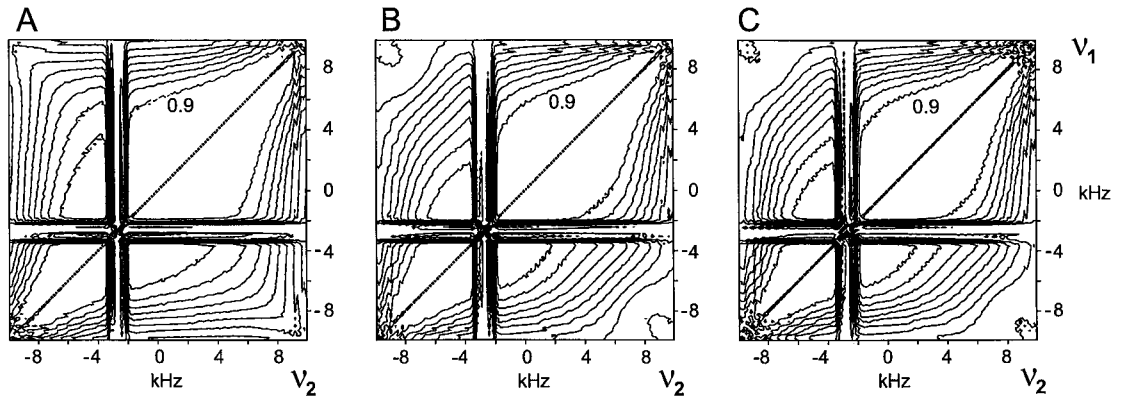

FIG. 3. Simulated offset dependence of the transfer efficiency (*4*, *23*) of (A) *x*, (B) *y*, and (C) z magnetization for an isolated two-spin system under sequence D of Fig. 1 with selective pulses applied at −2.7116 kHz using Gaussian $90^\circ_\varphi(3)$ pulses with a duration of 1.844 ms. The level increment is 0.1 and the highest contour level is 0.9.

not covered by the selective 90° pulses of the COIN sequence and hence were not decoupled during the mixing period.

In summary, the COIN experiment presented provides a flexible and efficient experimental approach to reduce the effective size of coupled spin systems during isotropic mixing experiments. The experiment yields isotropic coherence and polarization transfer that allows for the first time one to combine the superior transfer efficiency of tailored correlation spectroscopy (TACSY) experiments with standard sensitivity-enhancement techniques. The new approach relies on two avaraging processes.

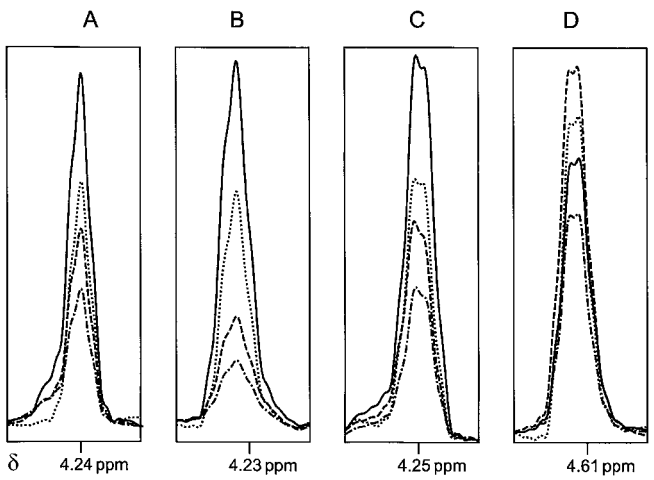

FIG. 4. Traces of NH–H_α cross peaks of the (A) Leu, (B) Ala, (C) Arg, and (D) Tyr residues of the peptide Gln-Lys-Leu-Glu-Ala-Met-His-Arg-Gln-Lys-Tyr-Pro. The solid curves correspond to traces of the sensitivity-enhanced TACSY spectrum using the COIN mixing sequence shown in Fig. 1D and a mixing time of 73.7 ms. The dashed and dashed-dotted curves represent sensitivity-enhanced TOCSY experiments with a mixing period of 44.9 and 58.7 ms, respectively. The dotted curves represent traces the HNHA-TACSY experiment using the CABBY-1 sequence (*6*) with a mixing time of 60.7 ms (*6*). As this mixing sequence allows only the transfer of a single magnetization component, no sensitivity enhancement was possible and the experimental traces were multiplied by a factor of $\sqrt{2}$ for comparison.

In a first (fast) averaging process broadband isotropic mixing conditions are created using well-known pulse sequences, such as DIPSI-2. In a second (slow) averaging process, selected couplings are removed by applying carefully phase-cycled selective pulses to a chosen frequency range. As the large offset terms of the free evolution Hamiltonian are already eliminated by the first averaging process, the second averaging process can be adequately described using a zero-order average Hamiltonian approach. The modular construction of the COIN experiment makes it possible to freely choose the desired active and nonactive frequency ranges by selecting the parameters of appropriate band-selective 90° pulses from a large pool of known pulse shapes (*26*). This is in contrast to the CABBY sequences (*6*) which require the computer optimization of a new multiple-pulse sequence if a different set of offset ranges is required for a given application. For simplicity, the COIN TACSY experiment was demonstrated experimentally for linear coupling networks, but it can also be applied to more general coupling topologies.

REFERENCES

1. S. R. Hartmann and E. L. Hahn, Nuclear double resonance in the rotating frame, *Phys. Rev.* **128,** 2042–2053 (1962).
2. L. Braunschweiler and R. R. Ernst, Coherence transfer by isotropic mixing: Application to proton correlation spectroscopy, *J. Magn. Reson.* **53,** 521 (1983).
3. A. Bax and D. G. Davis, MLEV-17-based two-dimensional homonuclear magnetization transfer spectroscopy, *J. Magn. Reson.* **65,** 355 (1985).
4. S. J. Glaser and J. J. Quant, Homonuclear and heteronuclear Hartmann–Hahn transfer in isotropic liquids, *in* "Advances in Magnetic and Optical Resonance" (W. S. Warren, Ed.), Vol. 19, pp. 59–252, Academic Press, San Diego (1996).
5. S. J. Glaser, Coupling topology dependence of polarization-transfer efficiency in TOCSY and TACSY experiments, *J. Magn. Reson. A* **104,** 283–301 (1993).
6. J. Quant, T. Prasch, S. Ihringer, and S. J. Glaser, Tailored correlation spectroscopy for the enhancement of fingerprint cross peaks in peptides and proteins, *J. Magn. Reson. B* **106,** 116–121 (1995).

7. T. Carlomagno, M. Maurer, M. Sattler, M. G. Schwendinger, S. J. Glaser, and C. Griesinger, PLUSH TACSY: Homonuclear planar TACSY with two-band selective shaped pulses applied to $C_\alpha C'$ transfer and C_β, $C^{aromatic}$ correlations, *J. Biomol. NMR* **8,** 161–170 (1996).
8. P. Schmidt, H. Schwalbe, S. J. Glaser, and C. Griesinger, Exclusive tailored correlation spectroscopy (E. TACSY), *J. Magn. Reson. B* **101,** 328–332 (1993).
9. D. Abramovich, S. Vega, J. Quant, and S. J. Glaser, The Floquet description of TOCSY and E. TACSY experiments, *J. Magn. Reson. A* **115,** 222–229 (1995).
10. S. J. Glaser and G. Drobny, The tailored TOCSY experiment: Chemical shift selective coherence transfer, *Chem. Phys. Lett*. **164,** 456–462 (1989).
11. S. J. Glaser and G. P. Drobny, Controlled coherence transfer by a multiple-step tailored TOCSY experiment, *Chem. Phys. Lett*. **184,** 553–559 (1991).
12. E̅. Kupče and R. Freeman, Stepwise propagation of coherence along a chain of atoms: DAISY-2, *J. Magn. Reson.* **100,** 208–214 (1992).
13. A. Mohebbi and A. J. Shaka, Selective homonuclear cross polarization, *J. Magn. Reson*. **94,** 204–208 (1991).
14. R. Konrat, I. Burghardt, and G. Bodenhausen, Coherence transfer in nuclear magnetic resonance by selective homonuclear Hartmann–Hahn correlation spectroscopy, *J. Am. Chem. Soc*. **113,** 9135–9140 (1991).
15. E̅. Kupče and R. Freeman, Multiple-Hartmann–Hahn coherence transfer in nuclear magnetic resonance spectroscopy, *J. Am. Chem. Soc*. **114,** 10671–10672 (1992).
16. J. Cavanagh and M. Rance, Sensitivity improvement in isotropic mixing (TOCSY) experiments, *J. Magn. Reson*. **88,** 72–85 (1990).
17. A. J. Shaka, C. J. Lee, and A. Pines, Iterative schemes for bilinear operators; application to spin decoupling, *J. Magn. Reson*. **77,** 274–293 (1988).
18. R. R. Ernst, G. Bodenhausen, and A. Wokaun, "Principles of Nuclear Magnetic Resonance in One and Two Dimensions," Oxford Univ. Press, Oxford (1987).
19. U. Haeberlen, "Advances in Magnetic Resonance" (J. S. Waugh, Ed.), Suppl. 1, Academic Press, New York (1976).
20. A. A. Maudsley, Modified Carr–Purcell–Meiboom–Gill sequences for NMR Fourier imaging applications, *J. Magn. Reson*. **69,** 488–491 (1986).
21. T. Gullion, D. B. Baker, and M. S. Conradi, New, compensated Carr–Purcell sequences, *J. Magn. Reson*. **89,** 479–484 (1990).
22. A. J. Shaka and A. Pines, Symmetric phase-alternating composite pulses, *J. Magn. Reson*. **71,** 495–503 (1987).
23. S. J. Glaser and G. P. Drobny, Assessment and optimization of pulse sequences for homonuclear isotropic mixing, *in* "Advances in Magnetic Resonance" (W. S. Warren, Ed.), Vol. 14, p. 35, Academic Press, New York (1990).
24. E̅. Kupče, J. Boyd, and I. D. Campbell, Short selective pulses for biochemical applications, *J. Magn. Reson. B* **106,** 300–303 (1995).
25. A. H. Sinclair, P. Berta, M. S. Palmer, J. R. Hawkins, B. L. Griffiths, M. J. Smith, J. W. Foster, A.-M. Frischauf, R. Lovell-Badge, and P. N. Goodfellow, A gene from the human sex-determining region encodes a protein with homology to a conserved DNA-binding motif, *Nature* **346,** 240–244 (1990).
26. W. R. Croasmun and R. M. K. Carlson, "Two-Dimensional NMR Spectroscopy," VCH, New York (1994).